Proc. Natl. Acad. Sci. USA
Vol. 94, pp. 11923–11928, October 1997
Biophysics

Effects of extracellular Ca^{2+} concentration on hair-bundle stiffness and gating-spring integrity in hair cells

ROBERT E. MARQUIS* AND A. J. HUDSPETH†

Howard Hughes Medical Institute and Laboratory of Sensory Neuroscience, The Rockefeller University, 1230 York Avenue, New York, NY 10021-6399

Contributed by A. J. Hudspeth, September 2, 1997

ABSTRACT **When a hair cell is stimulated by positive deflection of its hair bundle, increased tension in gating springs opens transduction channels, permitting cations to enter stereocilia and depolarize the cell. Ca^{2+} is thought to be required in mechanoelectrical transduction, for exposure of hair bundles to Ca^{2+} chelators eliminates responsiveness by disrupting tip links, filamentous interstereociliary connections that probably are the gating springs. Ca^{2+} also participates in adaptation to stimuli by controlling the activity of a molecular motor that sets gating-spring tension. Using a flexible glass fiber to measure hair-bundle stiffness, we investigated the effect of Ca^{2+} concentration on stiffness before and after the disruption of gating springs. The stiffness of intact hair bundles depended nonmonotonically on the extracellular Ca^{2+} concentration; the maximal stiffness of $\approx$1200 $\mu N \cdot m^{-1}$ occurred when bundles were bathed in solutions containing 250 μM Ca^{2+}, approximately the concentration found in frog endolymph. For cells exposed to solutions with sufficient chelator capacity to reduce the Ca^{2+} concentration below $\approx$100 nM, hair-bundle stiffness fell to $\approx$200 $\mu N \cdot m^{-1}$ and no longer exhibited Ca^{2+}-dependent changes. Because cells so treated lost mechanoelectrical transduction, we attribute the reduction in bundle stiffness to tip-link disruption. The results indicate that gating springs are not linearly elastic; instead, they stiffen with increased strain, which rises with adaptation-motor activity at the physiological extracellular Ca^{2+} concentration.**

The hair bundle of the vertebrate hair cell transduces mechanical stimuli, such as sounds and accelerations, into electrical signals. In the bullfrog's sacculus, the hair bundle comprises $\approx$60 stereocilia and a single kinocilium (1). A stereocilium is not a true cilium but contains a highly cross-linked, paracrystalline array of actin filaments (2) that confers a high flexural rigidity (3, 4). Each stereocilium tapers at its base, reducing the number of actin filaments at its insertion into the hair cell's apical surface (1). Deflection of the bundle therefore causes a stereocilium to pivot about its insertion rather than to flex along its length. The spring constant of the pivot accords with the number and flexural rigidity of the actin filaments at the insertion (3–5).

Mechanoelectrical transduction is initiated by deflection of the hair bundle (reviewed in ref. 6). During positive stimulation, shear between stereocilia tenses the gating springs that control the activity of transduction channels (7); increased gating-spring tension opens channels and allows cations, dominantly K^+ but also Ca^{2+}, to enter the stereocilia. By contrast, the decrease in gating-spring tension that accompanies negative stimulation favors transduction-channel closure. A gating spring is probably a tip link (8), an extracellular filament that interconnects two stereocilia along the bundle's axis of maximal sensitivity. Support for this identity comes from studies in which hair cells are treated with tetracarboxylate Ca^{2+} chelators, which both eliminate transduction (9–11) and disrupt tip links (12, 13). Moreover, cultured hair cells regain transduction as tip links reappear (14).

Hair-cell adaptation is a mechanical process thought to involve the restoration of gating-spring tension toward the resting level during sustained stimulation (15). Ca^{2+} evidently regulates the activity of a molecular motor, perhaps comprising myosin Iβ molecules, which is coupled to the gating spring (reviewed in ref. 16). During a positive stimulus, Ca^{2+} enters through an open transduction channel and allows the adaptation motor to slide down the stereocilium; this movement decreases tension in the gating spring and allows channels to reclose. By contrast, a negative stimulus lowers the intracellular Ca^{2+} concentration in the vicinity of transduction channels (17), promotes motor climbing, and thus increases gating-spring tension. Ca^{2+} likely exerts its effect on the motor by binding to calmodulin light chains on the myosin molecules and regulating their activity (18).

The extracellular Ca^{2+} concentration controls the rate and extent of adaptation in the hair cell (11, 19, 20) by affecting the Ca^{2+} influx through transduction channels and modulating the activity of adaptation motors (15, 21). The Ca^{2+} concentration also determines the channels' resting open probability, which increases from $\approx$0.1 in 2.8 mM Ca^{2+} to $>$0.5 in 50 μM Ca^{2+} (7, 11, 22). Reasoning that adaptation involves adjustments of gating-spring tension, we have sought mechanical changes in hair bundles associated with Ca^{2+}-regulated adjustments of gating-spring tension.

METHODS

Experimental Preparation and Saline Solutions. Experiments were conducted on saccular hair cells of the bullfrog, *Rana catesbeiana*. The saccular macula was dissected and maintained at room temperature in oxygenated standard saline solution containing 110 mM Na^+, 2 mM K^+, 4 mM Ca^{2+}, 118 mM Cl^-, 3 mM D-glucose, and 5 mM Hepes (pH 7.25). Unless otherwise indicated, chemicals were obtained from Sigma.

Low-Ca^{2+}-concentration saline solutions were prepared in plastic containers with deionized water to which no divalent cations were added. The stock no-added-Ca^{2+} saline solution (NACSS) contained 110 mM Na^+, 2 mM K^+, 110 mM Cl^-, 3 mM D-glucose, and 5 mM Hepes (pH 7.25). Ca^{2+} chelators were employed in two ways. For some experiments, NACSS was passed over a 1,2-bis(2-aminophenoxy)ethane-*N*,*N*,*N*′,*N*′-tetraacetic acid (BAPTA)–polystyrene column (BPS; Molec-

Abbreviations: BAPTA, 1,2-bis(2-aminophenoxy)ethane-*N*,*N*,*N*′,*N*′-tetraacetic acid; NACSS, no-added-Ca^{2+} saline solution.

*Present address: Medical Scientist Training Program, University of Texas Southwestern Medical Center, Dallas, TX 75235-9117.

†To whom reprint requests should be addressed at: Howard Hughes Medical Institute and Laboratory of Sensory Neuroscience, Box 314, The Rockefeller University, 1230 York Avenue, New York NY 10021-6399. e-mail: hudspaj@rockvax.rockefeller.edu.

The publication costs of this article were defrayed in part by page charge payment. This article must therefore be hereby marked "*advertisement*" in accordance with 18 U.S.C. §1734 solely to indicate this fact.

ular Probes) to remove Ca^{2+}. This procedure reduced the Ca^{2+} concentration to ≈300 nM, as determined with a Ca^{2+}-selective electrode (Orion Research, Boston). Alternatively, one of the Ca^{2+} chelators EDTA, EGTA, BAPTA (or one of its derivatives, all from Molecular Probes), arsenazo III, or antipyrylazo III was added to NACSS at the concentration shown in Table 1.

Hair-Bundle Stiffness Measurements. For hair-bundle stiffness and receptor-potential measurements from individual hair cells, we used a published variant of the force–fiber technique and conventional microelectrode methods (23). The isolated saccular macula was incubated for 15–240 min in standard saline solution containing 10–50 mg·liter^{-1} subtilopeptidase (type VIII, IX, or XXIV). After the otolithic membrane had been removed with an eyelash, the macula was secured to the coverslip bottom of a 500-μl chamber and bathed in oxygenated standard or experimental saline solution.

Hair cells were visualized with a ×40, water-immersion objective lens of numerical aperture 0.75 on an upright microscope (MPS, Carl Zeiss). A dual photodiode (UV-140-2, EG & G Electro-Optics, Salem, MA) mounted at the microscope's camera port permitted us to detect fiber-tip and hair-bundle displacements with a sensitivity of ≈1 nm (15). Signals from the photodiode were filtered with an eight-pole Bessel filter whose half-power frequency was set at 1–5 kHz; the signals were digitized and recorded at a sampling frequency of 2.5–12.5 kHz with a computer (Quadra 800, Apple Computer, Cupertino, CA) programmed in LABVIEW (version 3.1, National Instruments, Austin, TX).

Stimulus fibers, fabricated by reducing borosilicate glass rods 1.2 mm in diameter (Kimble KG-33; Garner Glass, Claremont, CA), were mounted horizontally on a stack-type piezoelectric actuator (P835.10, Physik Instrumente, Waldbronn, Germany). Driving signals for the stimulus actuator were supplied by the computer and low-pass filtered at 1.0–1.5 kHz. Each stimulus fiber was characterized by measuring the Brownian motion of its tip in water. From the power spectrum of this motion, we determined the fiber's stiffness, 200-1000 μN·m^{-1}, and its viscous drag coefficient, 40–300 nN·s·m^{-1}.

Measurements of Mechanoelectrical Transduction. Because we wished to measure the stiffness of hair bundles exclusively for cells whose transduction was initially intact, we monitored receptor potentials by conventional microelectrode techniques. Microelectrodes were fabricated with an electrode puller (P-80/PC; Sutter Instruments, Novato, CA) such that their resistances were 100–300 MΩ when filled with 3 M KCl and 10 mM glycylglycine at pH 8.5. To facilitate access to the apical cellular surface adjacent to the bundle's short edge, electrodes were bent ≈60° from the shank's axis at ≈300 μm from their tips (24). A direct-coupled amplifier set to a pass band of 0–1 kHz (Axoclamp-2A; Axon Instruments, Foster City, CA) measured the cell's membrane potential; the output signal was filtered and sampled at the frequencies used for the photodiode signals.

While individual hair bundles of hair cells near the abneural margin of the macula were stimulated with flexible glass fibers, the resultant receptor potentials were measured. Responses were first recorded with the preparation bathed in standard saline solution, after which the bath was exchanged by manual perfusion with a test solution (Table 1). Preparations were used only when >75% of the cells exhibited normal hair-bundle morphology, resting potentials more negative than −40 mV, and sensitive mechanoelectrical transduction in standard saline solution. Because satisfactory electrode penetrations were difficult to obtain with <1 mM extracellular Ca^{2+}, receptor potentials were recorded with the preparation bathed in standard saline solution before and after exposure to such solutions. Preparations that had deteriorated in low-Ca^{2+} solutions were excluded from subsequent analysis.

We measured each hair bundle's instantaneous displacement during the 0.75–1.25 ms after the onset of displacement. We chose this interval, which corresponded to the maximal bundle excursion during the bundle's mechanical twitch (23), to remain consistent with previous work (25). From these displacement measurements and knowledge of the fiber's calibrated stiffness, we determined each bundle's instantaneous slope and chord stiffnesses (25, 26). By measuring the bundle's displacement during the final 10 ms of the step, we also determined its static chord stiffness after adaptation had brought the bundle's position to a steady state.

To measure the summated receptor currents of hair cells, we used previously described methods to record the transepithelial current in a two-chamber apparatus (27, 28). We stimulated hair cells *en masse* with a solid glass probe ≈400 μm in

Table 1. Effects of Ca^{2+} chelators on transepithelial current

Saline solution	Chelator concentration	K_d	Total [Ca^{2+}]	Calculated free [Ca^{2+}]	Measured [Ca^{2+}]	Normalized recovery	n
Standard saline solution (SSS)			4 mM	4 mM	4 mM	1.08 ± 0.12	4
SSS with BAPTA	3 mM	160 nM	4 mM	1 mM	1 mM	1.12 ± 0.28	5
SSS with EGTA	3 mM	96 nM	4 mM	1 mM	1 mM	0.95 ± 0.12	6
200 μM Ca^{2+} saline solution			200 μM	200 μM	200 μM	1.21 ± 0.01	2
NACSS					710 ± 30 nM	1.12 ± 0.28	14
5,5′-Dinitro-BAPTA in NACSS	5 mM	20 mM	≈1 μM	0.8 μM		0.99 ± 0.31	3
BPS-treated NACSS					270 ± 20 nM	0.87 ± 0.24	8
Arsenazo III in NACSS	1 mM	35 μM	≈9 μM	296 nM	150 ± 6 nM	0.94 ± 0.08	5
BAPTA with 350 μM Ca^{2+}	1 mM	160 nM	350 μM	86 nM	81 ± 3 nM	0.47 ± 0.14	2
5-Nitro-BAPTA in NACSS	1 mM	94 μM	≈1 μM	86 nM	110 ± 6 nM	0.80 ± 0.18	5
5-Nitro-BAPTA in NACSS	5 mM	94 μM	≈1 μM	18 nM		0.04 ± 0.05	2
Antipyrylazo III in NACSS	5 mM	40 nM	≈9 μM	14 nM	37 ± 2 nM	0.94 ± 0.04	2
4,4′-Difluoro-BAPTA in NACSS	5 mM	4.6 μM	≈1 μM	900 pM		0.02	1
5,5′-Dibromo-BAPTA in NACSS	5 mM	3.6 μM	≈1 μM	700 pM		0.01 ± 0.02	2
BAPTA in NACSS	5 mM	160 nM	≈1 μM	30 pM		0.02 ± 0.02	4
EGTA in NACSS	5 mM	96 nM	≈1 μM	20 pM		0.08 ± 0.08	3
5,5′-Dimethyl-BAPTA in NACSS	5 mM	40 nM	≈1 μM	8 pM		0.04 ± 0.03	2
EDTA in NACSS	5 mM	25 nM	≈1 μM	5 pM		0.04 ± 0.05	2

Values for the dissociation constants (K_d) for EGTA and EDTA in solutions of pH 7.25 were calculated according to the methods of Blinks *et al*. (ref. 32, pp. 109–112) using rate constants from Martell and Smith (33); K_d values for the other chelators were taken directly from the literature. Free Ca^{2+} concentrations were calculated and in some cases measured with a Ca^{2+}-selective electrode; measurements of solutions with nanomolar free Ca^{2+} concentrations were repeated five times. The normalized recovery represents the fraction of each control receptor current recovered after replacement of the test solution with standard saline solution. Values are given as means ± SD.

tip diameter. In some experiments, the otolithic membrane was partially peeled from the underlying macula so that only similarly oriented hair cells were stimulated (27). After the probe had been lowered onto the otolithic membrane, displacement pulses of ≈1 μm were delivered with a piezoelectric bimorph stimulator. The voltage-clamp amplifier reported the transepithelial current necessary to cancel the summed receptor currents of the stimulated cells. The signals sent to the stimulator and those sampled from the amplifier were respectively supplied and recorded by the computer and software described. Stimuli were low-pass filtered at 0.35 kHz and transepithelial currents were filtered at 1 kHz.

The peak current was first determined with standard saline solution in both chambers. After exchange of at least 10 volumes of an experimental saline solution in the upper chamber, the peak current remaining after the solution change was recorded. Although tight junctions can dissociate upon exposure to low-Ca^{2+} solutions (29, 30), the transepithelial resistance is not significantly affected when such a solution is placed in only the upper compartment of the experimental chamber (28). We therefore believe that our receptor-current measurements were not compromised by failure of the voltage-clamp amplifier to operate with a leaky epithelium.

RESULTS

Hair-Bundle Stiffness. We determined the stiffness of individual hair bundles by deflecting them with a calibrated, flexible glass fiber (3, 4, 15, 23, 25). By measuring a bundle's displacement 0.75–1.25 ms after the onset of stimulation, we could ascertain its dynamic slope stiffness (Fig. 1*D*) and chord stiffness (Fig. 1*E*). The static stiffness (Fig. 2) was assayed by measuring the bundle's displacement during the last 10 ms of a pulse, after the adaptive mechanical relaxation. Cellular integrity was signaled by active hair-bundle twitches, gating compliance, and mechanical relaxation associated with adaptation (Fig. 1*B*; refs. 15, 23, 25, and 31). To ensure the quality of mechanoelectrical transduction, we additionally monitored receptor potentials with conventional microelectrode techniques (Fig. 1*C*).

Each experiment was preceded by control measurements with the preparation bathed in standard saline solution containing 4 mM Ca^{2+}. After exchanging an experimental solution into the chamber by manual perfusion, we measured the stiffness of several bundles. Finally, to determine whether the cells remained healthy and transduction intact, we restored standard saline solution and determined the stiffness of additional bundles.

Both static and dynamic hair-bundle stiffnesses were maximal at a Ca^{2+} concentration of 250 μM (Fig. 2), the approximate concentration experienced by frog saccular hair bundles bathed in endolymph *in vivo* (7). Comparison of the stiffness measured in 250 μM Ca^{2+} saline solution to those at five other Ca^{2+} concentrations revealed significant differences in all instances (Student's two-tailed *t* tests; $P < 0.005$). Because we

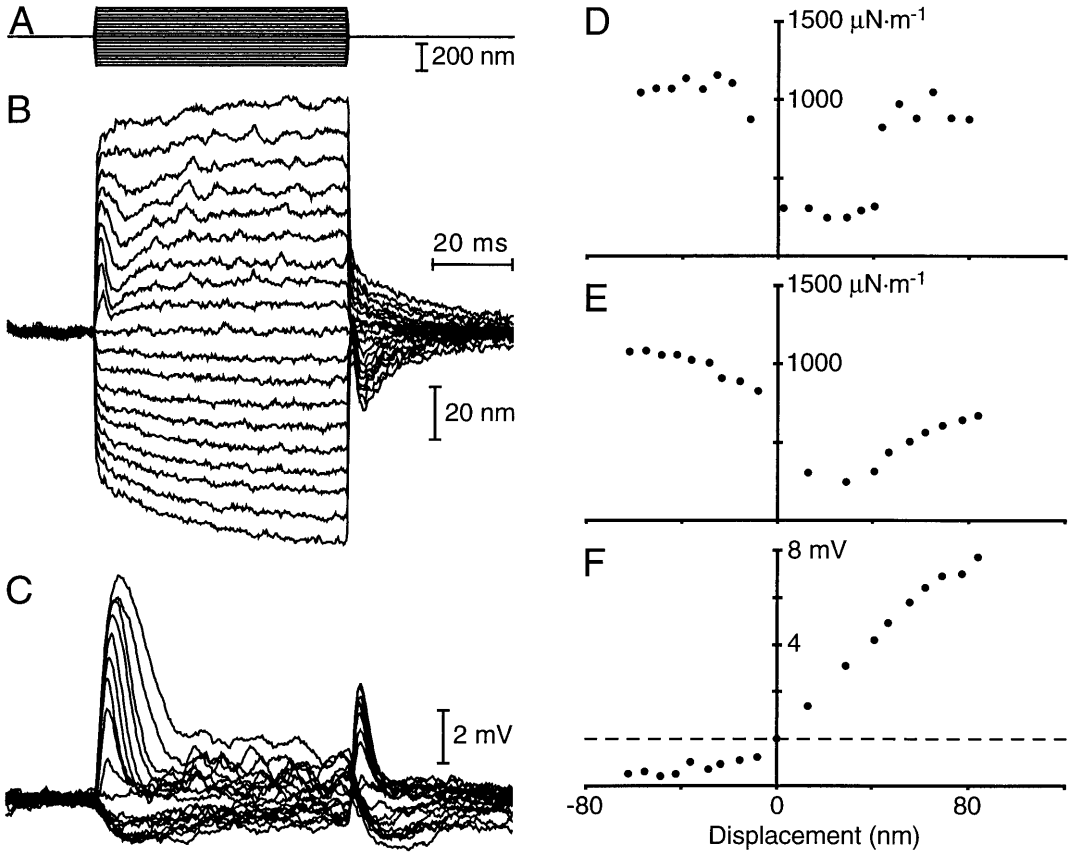

FIG. 1. Hair-bundle stiffness measurements. (*A*) A hair bundle was stimulated with a set of 19 displacement pulses whose amplitudes ranged from −200 nm to +200 nm. These 60-ms pulses were delivered to the base of a flexible fiber of stiffness 454 $\mu N \cdot m^{-1}$, whose tip was attached to the bundle. (*B*) The hair bundle's averaged mechanical responses to 10 stimulus sets in standard saline solution displayed two prominent features: mechanical twitches at the onsets of the positively directed stimuli, and slower, exponential relaxations indicative of adaptation. The bundle's instantaneous stiffness, measured during the first 0.75–1.25 ms of each stimulus pulse, averaged 754 $\mu N \cdot m^{-1}$ over all of the stimuli. The static stiffness, measured during the last 10 ms of each pulse, averaged 564 $\mu N \cdot m^{-1}$. (*C*) The cell's receptor potentials, recorded simultaneously with the mechanical responses, displayed depolarizing transients associated with bundle twitches. The peak depolarization was 7.7 mV from the cell's resting potential of −44 mV. (*D*) The bundle's slope stiffness declined near the bundle's resting position, the phenomenon of gating compliance. (*E*) The chord stiffness revealed a similar local minimum. (*F*) The relation between peak receptor potential and displacement characterized the hair bundle's mechanical sensitivity.

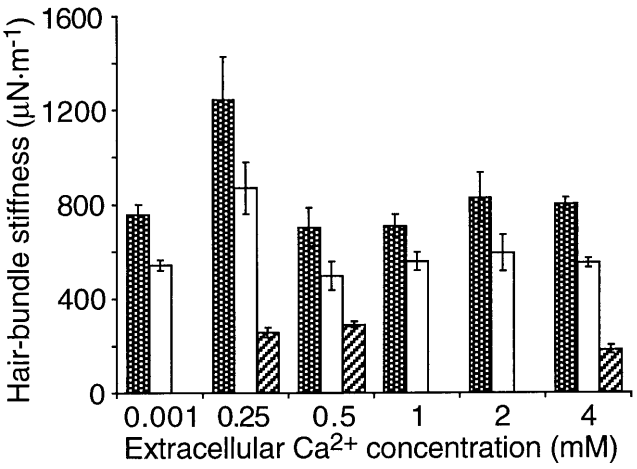

FIG. 2. Dependence of hair-bundle stiffness on extracellular Ca^{2+} concentration. The average instantaneous (dark filled bars) and static (open bars) chord stiffnesses are plotted for six Ca^{2+} concentrations. The error bars represent standard errors of the means. Note that hair-bundle stiffness was maximal when the cells' apical surfaces were bathed in a solution whose Ca^{2+} concentration resembled that of endolymph. Some bundles were treated with 5 mM BAPTA to disrupt tip links; their static stiffnesses (diagonally striped bars) were subsequently measured in Ca^{2+} concentrations of 0.25 mM, 0.5 mM, and 4 mM. These bundles displayed uniformly low stiffnesses independent of the Ca^{2+} concentration. The numbers of untreated cells analyzed at each Ca^{2+} concentration were as follows: 8 cells at 1 μM Ca^{2+}; 17 cells at 250 μM Ca^{2+}; 13 cells at 500 μM Ca^{2+}; 19 cells at 1 mM Ca^{2+}; 10 cells at 2 mM Ca^{2+}; and 307 cells at 4 mM Ca^{2+}. The numbers of cells analyzed after BAPTA treatment were as follows: 8 cells at 250 μM Ca^{2+}; 4 cells at 500 μM Ca^{2+}; and 8 cells at 4 mM Ca^{2+}.

suspected that the increased stiffness at 250 μM Ca^{2+} was directly associated with the transduction machinery, we disrupted gating springs and remeasured bundle stiffness at three Ca^{2+} concentrations. Bundles treated with 5 mM BAPTA became 4-fold as compliant as untreated bundles and subsequently exhibited neither Ca^{2+}-dependent stiffness changes (Fig. 2) nor mechanoelectrical transduction (Fig. 3).

Gating-Spring Integrity. To test for gating-spring integrity after exposure of hair bundles to various Ca^{2+} concentrations and Ca^{2+} chelators, we assayed mechanoelectrical transduction by measuring transepithelial receptor currents and by recording receptor potentials from individual hair cells. In each instance, we recorded responses before and after manually substituting at least 10 chamber volumes of experimental solution.

In the transepithelial-current assay, mechanoelectrical transduction was unaffected after hair bundles had been exposed to chelator-free solutions containing low Ca^{2+} concentrations (Table 1). Solutions prepared without the addition of divalent cations had a Ca^{2+} concentration of 710 ± 30 nM (n = 5) as measured with a Ca^{2+}-selective electrode. As a conservative estimate, and to facilitate calculations, we assumed that such solutions contained 1 μM Ca^{2+} (Table 1). When these solutions were passed over a BAPTA–polystyrene column, their Ca^{2+} concentration was reduced to 270 ± 20 nM (n = 5); the treated solutions nevertheless did not disrupt transduction or diminish bundle stiffness.

The $CaCO_3$ crystals on the otolithic membrane might have provided a source of Ca^{2+} that locally elevated its concentration in experimental solutions and thereby preserved transduction. To eliminate this possibility, we repeated the low-Ca^{2+} treatments on preparations from which the otolithic membranes had been removed and assayed transduction in individual hair cells. After 15-min incubations in chelator-free solutions of low Ca^{2+} concentration, hair cells manifested normal receptor potentials, twitches, and adaptation (Fig. 3*B*).

Transepithelial recordings demonstrated that transduction was also preserved after treatments with low-Ca^{2+} solutions buffered with 5,5′-dinitro-BAPTA or the metallochromic Ca^{2+} indicators arsenazo III and antipyrylazo III (Table 1; refs. 32 and 34). In addition, receptor-potential measurements confirmed that transduction was intact in each of four cells after exposure to antipyrylazo III (data not shown). Solutions prepared with 1 mM 5-nitro-BAPTA, which had a calculated

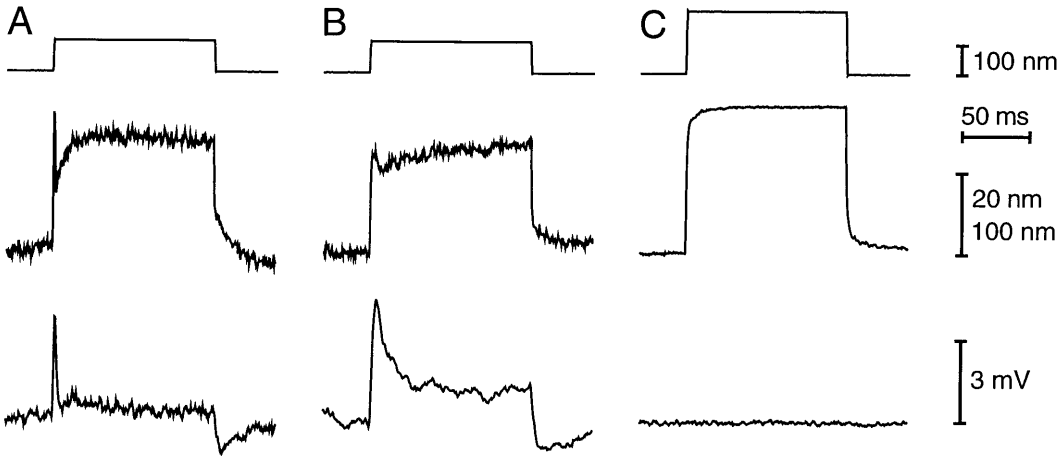

FIG. 3. Receptor-potential assays of tip-link integrity. (*A*) The top trace represents the 100-nm, 120-ms displacement pulse delivered to the base of a fiber of stiffness 184 μN·m^{-1}. The bundle's mechanical response is shown in the middle trace; the cell's receptor potential is displayed in the bottom trace. The preparation was bathed in standard saline solution containing 4 mM Ca^{2+}. Note the twitch in the mechanical record and the corresponding depolarizing spike in the receptor-potential record. The bundle's average instantaneous stiffness was 611 μN·m^{-1}. (*B*) Comparable measurements were taken from a hair cell in the sacculus contralateral to that of *A*, which had been incubated for 15 min in NACSS that had been passed over a BAPTA–polystyrene column to remove Ca^{2+}. The bundle produced a twitch and the cell displayed a healthy receptor potential in spite of the prior exposure to a Ca^{2+} concentration of only ≈300 nM. The bundle's average instantaneous stiffness was 724 μN·m^{-1}; the stimulus fiber and pulse size used were identical to those for *A*. Receptor potentials indicative of sensitive transduction were recorded from an additional 14 cells exposed to BAPTA–polystyrene-treated NACSS. (*C*) Receptor potentials were eliminated after a 5-min exposure to a solution containing 5 mM EGTA. This treatment also reduced the bundle's stiffness to 81 μN·m^{-1}. Transduction was eliminated and bundle stiffness reduced in each of 8 other cells treated with 5 mM EGTA; similar results were obtained for each of 29 cells treated with 5 mM BAPTA for 1–10 min. The bundle was displaced with a 200-nm stimulus of the same duration as in *A* and *B*; the probe's stiffness was 446 μN·m^{-1}. The 100-nm displacement calibration applies only to the middle trace of *C*.

free Ca^{2+} concentration of 86 nM, also spared transduction. A solution prepared with the identical free Ca^{2+} concentration, but buffered with 1 mM BAPTA to which 350 μM Ca^{2+} had been added, reduced the transepithelial receptor current by about half (Table 1).

Consistent with previous reports (11, 13), transepithelial receptor currents were eliminated by low-Ca^{2+} solutions prepared with the tetracarboxylate chelators EDTA, EGTA, BAPTA, and several of its derivatives. Receptor-potential measurements confirmed that transduction was consistently eliminated by exposure to low-Ca^{2+} solutions containing BAPTA and EGTA (Fig. 3*C*). In addition, hair-bundle twitches and the mechanical relaxation associated with adaptation were never observed after such treatments.

DISCUSSION

Our principal finding is that hair-bundle stiffness depends nonmonotonically on the extracellular Ca^{2+} concentration (Fig. 2). The dynamic stiffness reaches a maximal value near 1200 $\mu N \cdot m^{-1}$ when the extracellular Ca^{2+} concentration is 250 μM and is essentially constant at 750 $\mu N \cdot m^{-1}$ for other concentrations exceeding 1 μM. When the Ca^{2+} concentration is greatly reduced by the addition of certain tetracarboxylate Ca^{2+} chelators, the stiffness drops to 200 $\mu N \cdot m^{-1}$. We attribute this residual component to the stereociliary pivots in the absence of gating springs. The concomitant loss of transduction (Table 1 and Fig. 3*C*) and Ca^{2+} independence of bundle stiffness (Fig. 2) suggest that chelator exposure disrupts tip links and that the Ca^{2+} dependence of bundle stiffness resides in those structures.

Gating springs can slacken when a hair bundle undergoes a negative displacement (7, 25, 35); they evidently buckle under compression and cease to behave as linearly elastic elements. The present results indicate that gating springs also depart from linear elasticity when subjected to extension. When bundles are bathed in solutions with a physiological Ca^{2+} concentration, their stiffness reaches a maximal value. Relative to standard-saline conditions, the reduced extracellular Ca^{2+} concentration decreases Ca^{2+} entry into stereocilia and reduces the intracellular Ca^{2+} concentration, presumably promoting climbing activity by the adaptation motor and thus increasing gating-spring tension. If the gating springs were linearly elastic, a change in tension would not affect their stiffness. If their stiffness increases as a function of tension (36), however, then we would expect the observed increase in bundle stiffness. Because many elastic materials, both biological and synthetic, exhibit stiffening upon extension (37–39), it is not surprising that the gatings springs behave in this manner.

That hair-bundle stiffness depends nonmonotonically on the Ca^{2+} concentration is at once intriguing and perplexing. We might predict that the rate at which the adaptation motor climbs would increase further as the extracellular Ca^{2+} concentration falls below 250 μM, thus continuing to increase tip-link tension and therefore bundle stiffness. Our results show instead that, when the Ca^{2+} concentration is reduced to $\approx$1 μM, the stiffness falls to the level found in standard saline solution. This decrease is not due to tip-link disruption, for bundles exposed to this Ca^{2+} concentration continued to transduce (Table 1 and Fig. 3*B*). It seems most likely that gating-spring tension declines when the Ca^{2+} concentration is reduced below 250 μM.

One explanation is that force production by the adaptation motor is reduced by the lower Ca^{2+} concentration. The adaptation motor is regulated by calmodulin (18), whose affinity for myosin I is sensitive to the Ca^{2+} concentration (40). Furthermore, the ATPase activity of brush-border myosin I is halved as the Ca^{2+} concentration falls from 10 μM to 1 μM (40). It is therefore possible that, when a bundle is exposed to Ca^{2+} concentrations below the physiological range, the adaptation motor's activity declines. In support of this hypothesis, adaptation is inhibited by Ca^{2+} concentrations below 100 μM (11, 19).

The unexpectedly low hair-bundle stiffness achieved at 1 μM Ca^{2+} might alternatively reflect cellular damage. Morphological changes were not seen for several hours *post mortem* in preparations bathed in solutions containing >100 μM Ca^{2+}, but somatic vesiculation and edema were often observed within 30 min after substitution of NACSS. Although receptor-potential and transepithelial-current measurements revealed that transduction persisted after such treatments (Fig. 3*B* and Table 1), some pathological effect of the exposure to 1 μM Ca^{2+} might nevertheless have lowered the bundle stiffness.

Certain biological macromolecules exhibit a highly nonlinear stiffness that depends on strain; these and related molecules are accordingly candidates to constitute the tip link. The muscle protein titin, for example, displays linear elasticity and a low stiffness for small extensions, such that essentially all the energy stored during an extension is recoverable when the molecule shortens (41–43). By contrast, titin's stiffness increases exponentially with large strains, as its immunoglobin- and fibronectin III-like domains unfold. Its restoring force after large extensions is greatly diminished, however, so that the applied force must be greatly reduced before titin refolds: there is a pronounced hysteresis in the force–extension relationship for large strains. This characteristic renders titin itself a questionable tip-link candidate, for such substantial hysteresis has not been observed in hair bundles.

Another finding of this study is that hair bundles of the bullfrog's sacculus can be exposed to solutions with Ca^{2+} concentrations as low as 50–100 nM without damage to the transduction apparatus. Because chelators were needed to achieve Ca^{2+} concentrations <300 nM, we could not determine whether gating springs were disrupted by a lack of Ca^{2+} or by a direct effect of specific chelators. Some extracellular protein interactions, such as the binding of ligands to integrins and cadherins, are Ca^{2+}-dependent (reviewed in refs. 44 and 45), so it is plausible that the tip link's attachment to the insertional plaque similarly requires Ca^{2+}. On the other hand, Ca^{2+} chelators have been shown to bind to and alter the activity of various proteins (46, 47), so a direct effect of chelators on tip links is also possible. Whatever the mechanism of gating-spring disruption, the present results afford two alternatives to researchers wishing to study the machinery of mechanoelectrical transduction under low-Ca^{2+} conditions. First, one may use solutions passed over chelator columns; alternatively, one may employ solutions buffered with the metallochromic Ca^{2+} chelator arsenazo III or antipyrylazo III.

Our results confirm that a component of the transduction apparatus is sensitive to solutions prepared with Ca^{2+}-free chelators of the tetracarboxylate family (Table 1). Based on previous studies that correlated loss of transduction with disappearance of tip links on electron micrographs (13, 14), we presume that the tip link is the vulnerable component. This hypothesis is also supported by electron micrographs of hair bundles exposed to solutions of compositions identical to those that we used. Tip links are present when the chick's basilar papilla is incubated with BAPTA–polystyrene-treated solutions of low Ca^{2+} concentration, but they are eliminated by BAPTA-containing saline solutions (P. G. Gillespie, personal communication).

Previous studies have estimated that gating springs contribute approximately half of a hair bundle's total stiffness (15, 25, 26, 48). If the reduction in bundle stiffness after chelator exposure is wholly due to gating-spring disruption, however, our results suggest that gating springs account for 80% of the bundle's stiffness under physiological Ca^{2+} conditions (Fig. 2). This result indicates that a bundle may be very efficient at extracting the energy of a mechanical stimulus: if a majority of the bundle's stiffness resides in the gating springs, then most of

the work done on the bundle is directed there. A second implication of this result concerns active hair-bundle motions (Fig. 1*B*; refs. 3, 15, 23, 25, and 31), which may reflect changes in gating-spring tension. To effect signal amplification *in vivo*, these motions must be efficiently transmitted to an overlying accessory structure, such as an otolithic or tectorial membrane. The transfer of force would be optimized by gating springs that dominate the bundle's stiffness.

We thank Dr. P. G. Gillespie for scanning electron microscopic examination of specimens; he and members of our research group provided useful comments on the manuscript. This research was supported by National Institutes of Health Grant DC00241. A.J.H. is an Investigator of Howard Hughes Medical Institute.

1. Jacobs, R. A. & Hudspeth, A. J. (1990) *Cold Spring Harbor Symp. Quant. Biol.* **55,** 547–561.
2. Tilney, L. G., DeRosier, D. J. & Mulroy, M. J. (1980) *J. Cell Biol.* **86,** 244–259.
3. Crawford, A. C. & Fettiplace, R. (1985) *J. Physiol. (London)* **364,** 359–379.
4. Howard, J. & Ashmore, J. F. (1986) *Hear. Res.* **23,** 93–104.
5. Duncan, R. K. & Grant, J. W. (1997) *Hear. Res.* **104,** 15–26.
6. Hudspeth, A. J. (1989) *Nature (London)* **341,** 397–404.
7. Corey, D. P. & Hudspeth, A. J. (1983) *J. Neurosci.* **3,** 962–976.
8. Pickles, J. O., Comis, S. D. & Osborne, M. P. (1984) *Hear. Res.* **15,** 103–112.
9. Sand, O. (1975) *J. Comp. Physiol. A* **102,** 27–42.
10. Hudspeth, A. J. & Corey, D. P. (1977) *Proc. Natl. Acad. Sci. USA* **74,** 2407–2411.
11. Crawford, A. C., Evans, M. G. & Fettiplace, R. (1991) *J. Physiol. (London)* **434,** 369–398.
12. Neugebauer, D.-C. & Thurm, U. (1987) *Cell Tissue Res.* **249,** 199–207.
13. Assad, J. A., Shepherd, G. M. G. & Corey, D. P. (1991) *Neuron* **7,** 985–994.
14. Zhao, Y.-D., Yamoah, E. N. & Gillespie, P. G. (1996) *Proc. Natl. Acad. Sci. USA* **94,** 15469–15474.
15. Howard, J. & Hudspeth, A. J. (1987) *Proc. Natl. Acad. Sci. USA* **84,** 3064–3068.
16. Hudspeth, A. J. & Gillespie, P. G. (1994) *Neuron* **12,** 1–9.
17. Lumpkin, E. A. & Hudspeth, A. J. (1995) *Proc. Natl. Acad. Sci. USA* **92,** 10297–10301.
18. Walker, R. & Hudspeth, A. J. (1996) *Proc. Natl. Acad. Sci. USA* **93,** 2203–2207.
19. Eatock, R. A., Corey, D. P. & Hudspeth, A. J. (1987) *J. Neurosci.* **7,** 2821–2836.
20. Hacohen, N., Assad, J. A., Smith, W. J. & Corey, D. P. (1989) *J. Neurosci.* **9,** 3988–3997.
21. Assad, J. A. & Corey, D. P. (1992) *J. Neurosci.* **12,** 3291–3309.
22. Ricci, A. J. & Fettiplace, R. (1997) *J. Physiol. (London)* **501,** 111–124.
23. Benser, M. E., Marquis, R. E. & Hudspeth, A. J. (1996) *J. Neurosci.* **16,** 5629–5643.
24. Hudspeth, A. J. & Corey, D. P. (1978) *Am. J. Physiol.* **234,** C56–C57.
25. Howard, J. & Hudspeth, A. J. (1988) *Neuron* **1,** 189–199.
26. Hudspeth, A. J. (1992) in *Sensory Transduction*, eds. Corey, D. P. & Roper, S. D. (Rockefeller Univ. Press, New York), pp. 357–370.
27. Corey, D. P. & Hudspeth, A. J. (1983) *J. Neurosci.* **3,** 942–961.
28. Lumpkin, E. A., Marquis, R. E. & Hudspeth, A. J. (1997) *Proc. Natl. Acad. Sci. USA* **94,** 10997–11002.
29. Martinez-Palomo, A., Meza, I., Beaty, G. & Cereijido, M. (1980) *J. Cell Biol.* **87,** 736–745.
30. Citi, S. (1992) *J. Cell Biol.* **117,** 169–178.
31. Jaramillo, F., J. Howard & Hudspeth, A. J. (1990) in *The Mechanics and Biophysics of Hearing*, eds. Dallos, P., Geisler, C. D., Matthews, J. W., Ruggero, M. A. & Steele, C. R. (Springer, Berlin), pp. 26–33.
32. Blinks, J. R., Wier, W. G., Hess, P. & Prendergast, F. G. (1982) *Prog. Biophys. Mol. Biol.* **40,** 1–114.
33. Martell, A. E. & Smith, R. M. (1974) *Critical Stability Constants* (Plenum, New York, NY), Vol. 1, pp. 204, 269.
34. Baylor, S. M., Hollingsworth, S., Hui, C. S. & Quinta-Ferreira, M. E. (1986) *J. Physiol. (London)* **377,** 89–141.
35. Yamoah, E. N. & Gillespie, P. G. (1996) *Neuron* **17,** 523–533.
36. Fung, Y. C. (1993) *Biomechanics: Mechanical Properties of Living Tissues* (Springer, New York), 2nd Ed. pp. 269–293.
37. Jewell, B. R. & Wilkie, D. R. (1958) *J. Physiol. (London)* **143,** 515–540.
38. Fung, Y. C. B. (1967) *Am. J. Physiol.* **213,** 1532–1544.
39. Pinto, J. G. & Fung, Y. C. (1973) *J. Biomechanics* **6,** 617–630.
40. Swanljung-Collins, H. & Collins, J. H. (1991) *J. Biol. Chem.* **266,** 1312–1319.
41. Kellermayer, M. S. Z., Smith, S. B., Granzier, H. L. & Bustamante, C. (1997) *Science* **276,** 1112–1116.
42. Rief, M., Gautel, M., Oesterhelt, F., Fernandez, J. M. & Gaub, H. E. (1997) *Science* **276,** 1109–1112.
43. Tskhovrebova, L., Trinick, J., Sleep, J. A. & Simmons, R. M. (1997) *Nature (London)* **387,** 308–312.
44. Jessell, T. M. (1988) *Neuron* **1,** 3–13.
45. Hynes, R. O. (1992) *Cell* **69,** 11–25.
46. Richardson, A. & Taylor, C. W. (1993) *J. Biol. Chem.* **268,** 11528–11533.
47. Combettes, L., Hannaert-Merah, Z., Coquil, J.-F., Rousseau, C., Claret, M., Swillens, S. & Champeil, P. (1994) *J. Biol. Chem.* **269,** 17561–17571.
48. Jaramillo, F. & Hudspeth, A. J. (1993) *Proc. Natl. Acad. Sci. USA* **90,** 1330–1334.